Reference No. ICF1007090R

ISSUES IN FRACTURE TOUGHNESS AND R-CURVE BEHAVIOR OF PARTICLE REINFORCED METAL MATRIX COMPOSITES

B. S. Majumdar

Department of Materials and Metallurgical Engineering, New Mexico Tech
801 Leroy Place, Socorro, NM 87801

ABSTRACT

Different ASTM procedures were used to estimate the crack initiation toughness and R-curve behavior of SiC-particle reinforced aluminum matrix composites, with both macroscopically homogeneous and heterogeneous microstructures. Although the initiation toughness was similar, the crack resistance behavior varied over a wide range, depending upon the technique used to analyze the load-displacement-crack length data. Analysis showed that the cracks essentially grew under small-scale yielding (SSY) conditions. Aluminum particles had a greater influence on the steady state toughness than the initiation toughness. The implication of crack growth under SSY conditions is further analyzed in the context of development of many brittle systems (such as intermetallics), where an R-curve behavior is suggested as a remedy for low crack initiation toughness. A center cracked tension (CCT) geometry is used to establish that the modest R-curve behavior is of little value when such materials are used under load controlled conditions; i.e., instability occurs immediately on crack initiation, so that the R-curve effect is not realized. Tearing modulus (T) of these materials, as well as many intermetallics are close to unity. Results suggest that an order of magnitude increase in T is necessary before the R-curve behavior can be exploited in component design.

KEYWORDS

Fracture toughness, R-curve, Aluminum, particle, DRA, composite, stability, toughening

INTRODUCTION

Discontinuously reinforced aluminum (DRA) composites possess lower plane strain fracture toughness (K_{Ic} or J_{Ic}) than the aluminum alloys from which they are derived. Consequently, efforts are under way to understand failure mechanisms, and to devise methods to obtain toughness comparable to the Al-alloy matrix.

In this paper, we report results on a model 7093 Al-alloy composite reinforced with SiC particles. Note that the J_{Ic} of DRAs are quite sensitive to the heat treatment, and exhibit a trend of higher toughness with decreasing yield strength, similar to the matrix alloy. The current high strength DRA behaved similarly, and data are available in [1]. In addition to intrinsic toughening mechanisms, DRAs can also be tailored through an extrinsic approach [2]. One such method is to incorporate regions of pure Al or neat matrix alloy, which act as ductile ligaments during fracture. The effectiveness of this method of toughening of DRAs is discussed here. Preliminary data were reported earlier [3].

In this paper, we also focus attention on the engineering application of the R-curve characteristics in materials of limited toughness. This topic is relevant not only for DRAs, but also is important for advanced intermetallic alloys, which possess relatively low toughness (~10-20 $MPa.m^{1/2}$). Microstructural modifications in these systems often produce improved J-R curve, but the effect on the initiation toughness, K_{Ic}/J_{Ic}, is small. Anticipated applications of such

materials in structures are often under load controlled conditions, such as in a fan blade or a turbine blade. In these systems it is important to assess if modest R-curve gains through microstructural design will be adequate for the intended application. Frequently, there is a perceived notion that an R-curve behavior is an insurance against failure. The partially flawed logic is that a higher toughness value generated from the R-curve can be plugged in the stress intensity formula, to obtain a higher critical load or a larger critical crack length than that based on K_{Ic}/J_{Ic}. Clearly this is an incorrect approach, and stability issues must be considered. We report results from our stability analysis.

EXPERIMENTS

Two types of composites were considered in this investigation, and they were all fabricated at Alcoa. The control DRA consisted of 7093 aluminum alloy matrix (7 Zn, 2.2 Mg, 1.5 Cu, 0.14 Zr, 0.1 Ni wt.%,) reinforced with 15 vol.% of SiC particles (average particle size ~10 μm), and prepared through a powder metallurgy route. In addition to the control DRA, ductile phase toughened materials were fabricated with different volume fractions of pure Al particles. The constituents are indicated in Table 1. Two different sizes were considered: aluminum particles of 300 μm (designated small) and 10 mm size (designated large). The global volume fraction of SiC particles was maintained constant at 15 %, so that the presence of a larger volume fraction of Al particles implies that SiC volume fraction was higher in the reinforced region of the toughened composites. In this way, the elastic modulus was held approximately constant at approximately 90 GPa in all the microstructures. All the DRAs were subjected to an underaging (UA) treatment, involving solutionizing at 490 C/4h, water quench, followed by a 120 C/25 min. aging treatment.

Fracture toughness, J_{Ic}, and J-resistance curve of the materials were evaluated using ASTM E-813 and E-561 procedures, and it is shown later why the E-561 procedure is more appropriate for the materials considered here. The compact tension (CT) specimen geometry was employed, with a thickness (B) of 7.6 mm, a width (W) of 20.3 mm, and a notch length of 7.6 mm. All the CT specimens were fatigue precracked according to the standard ASTM procedures to an a/W ratio of approximately 0.5, where 'a' is the crack length.

RESULTS

Figure 1 (a) shows the SEM microstructure of the control DRA in the as-extruded condition and illustrates that the distribution of SiC particles in the aluminum matrix is fairly homogeneous. Figures 1 (b) illustrates the microstructure of ductile phase toughened DRA with small aluminum particles. The tensile properties of the composites are summarized in Table 1:

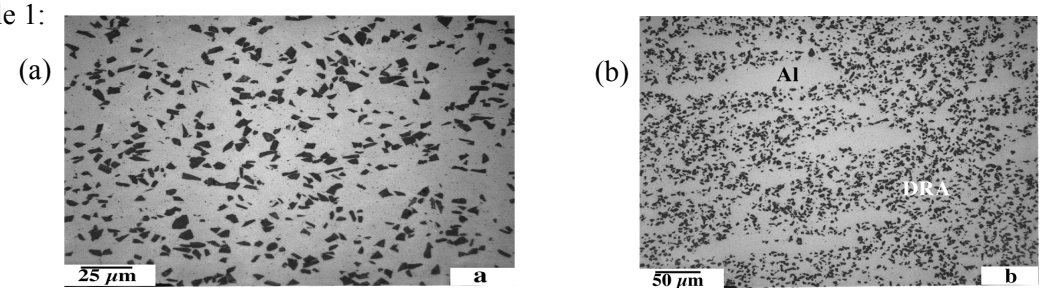

Figure 1. Microstructures of: (a) control DRA, and (b) DRA with 25% small Al-particles

TABLE 1. Results of tension and fracture toughness tests on the composites

Material	Yield Strength, MPa	Tensile Strength, MPa	Elongation, %	N, work hardening exponent	Initiation J_{Ic}, kJ/m^2	Initiation, $K_{a\text{-}eq}$, MPa.m$^{1/2}$	Steady State, K_{ss} MPa.m$^{1/2}$
Control DRA	503	629	5.9	0.089	2.9	16.0	20.0
DRA+10%large Al particles	436	555	4.4	0.087	3.0	16.5	25.2
DRA+25% small Al particles	453	546	4.4	0.075	5.0	24.0	34.6
DRA + 25% large Al particles	466	546	2.2	0.073	4.2	20.5	33.8

Initial analysis of the J-resistance (J-R) curve was conducted as per ASTM E-813, where

$$J_{pl} = \frac{2}{Bb}\int_0^{\Delta} Pd\Delta \qquad (1)$$

where Δ is the plastic part of the load-line displacement, B is the specimen thickness, and b is ligament width. ASTM E-1152 provides a slightly different equation to account for the history of crack growth. However, the difference was small, and did not appear to have a very significant effect on the J-R curve.

In order to assess the load-line displacement record, we used the EPRI estimation scheme of Kumar et al. [4,5] to estimate theoretically the plastic component of the total displacement. Plane strain formulation was used. Experimental data showed that the formulas from Kumar et al's [4,5] scheme severely overestimated the total displacement, by up to a factor of 10. Thus, these data confirmed that small scale yielding (SSY) was operative in our specimens. On the other hand, both ASTM E-813 and E-1152 owe their origin to the classical work of Rice and co-workers [6] who essentially assume full scale yielding of deeply notched specimens. In this work, we have attempted to solve this problem by deriving the J-R curve using the SSY formulation. In the spirit of Irwin's crack length correction approach, the measured displacements were used to derive an effective crack length. This was done by drawing a line from any point in the load-displacement record to the origin, and using the compliance formulas for the compact tension (CT) specimen to derive an effective crack length, a_{eq}. The standard LEFM formula was then used to compute K and hence J. This methodology is essentially what is used in ASTM E-561.

The K-resistance curves for the control DRA are compared in Figure 2, where the J values obtained through E-813 and

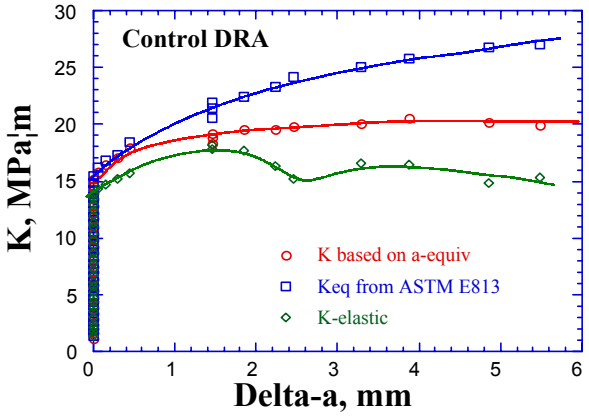

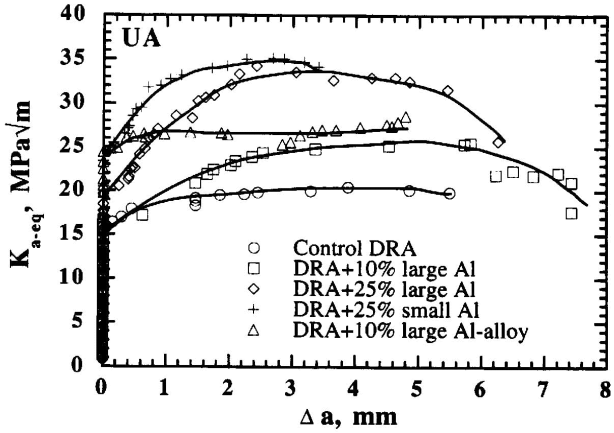

Figure 2. K-equivalent versus crack growth, Δa, using different ASTM procedures for the control DRA.

Figure 3. K-equivalent versus Δa using small-scale yielding approach. Results for the DRAs with different volume percent Al-particles are provided.

E1152 were converted to Ka-eq using Ka-eq=$\{JE/(1-\nu^2)\}^{1/2}$. Figure 2 shows that in the initial 0.5-1 mm of crack growth, the Ka-eq from ASTM E-813 and from the SSY formulation, are very similar. In fact, J_{Ic} results are nearly identical. However, the difference show up for crack growth beyond 1 mm. Figure 2 also shows that Keq based on SSY settles down to a *steady state* value of 20 MPa√m, whereas the data based on ASTM E-813 shows a continuously increasing trend.

The fracture surfaces did not reveal any difference in the crack morphology past the initial stretch zone (< 0.5 mm). Also, as already indicated, the plastic zone size was estimated to be of the order of 1 mm. Thus, there is very little reason why the growing crack should exhibit an ever-increasing trend beyond 1-2 mm of crack growth. The Ka-eq based on SSY indeed is consistent with the expectation of a steady state, K_{ss}, whereas that based on ASTM E-813 is not. Figure 2 also contains a plot of K_{el}, which is the elastic component of J. This plot does indicate drops, but the K value remains at around 15 MPa√m for the entire growth period. Thus, this can be considered with confidence as the lower limit value of K in predicting specimen instability, when previous details of loading are not known.

Figure 3 shows the Ka-eq resistance curves for the control DRA and DRAs containing Al particles in the UA condition. This plot shows that the initiation toughness for the ductile phase toughened materials are generally larger than the control DRA. The steady state toughness for the ductile phase toughened materials reveal a much greater improvement compared with the initiation toughness; an increase of as much as 70%.

MODELING OF FRACTURE TOUGHNESS AND STEADY STATE TOUGHNESS

In a previous paper [7] we modeled the fracture toughness of particulate reinforced composites, and showed that the toughness is quite sensitive to the constraint conditions. Assuming fracture to occur on attainment of a critical strain at one microstructural distance (equated to particle distance) ahead of the crack tip, the following formula was obtained:

$$K_{Ic} = 0.77\left\{\frac{\sigma_o \beta d E}{d_n(1-\nu^2)}\right\}^{1/2} v_p^{-1/6} \qquad (2)$$

where σ_o is the flow stress, v_p is the volume fraction of particles, d is the average particle diameter (10 μm here), and d_n represents the relation between crack tip opening displacement and J ($\delta = d_n J/\sigma_o$), and is given by $d_n = 0.78 - 2.73N + 3.065N^2$, where N is the work hardening exponent. β is 0.5 for a fully constrained crack (i.e., plane strain), and 0.91 for plane stress. Using the material constituent properties (E~90 GPa) and β=0.5, the predicted toughness for the control DRA material in the UA condition (σ_o=503 MPa) is 18.7 MPam$^{1/2}$, which compares favorably with the experimental data. In a separate publication [8], we reported the toughness for a thin specimen (0.76 mm thick) to be 31 MPa.m$^{1/2}$. Using β=0.91 instead of 0.5, the corresponding predicted plane stress toughness is 25.2 MPa.m$^{1/2}$, which is slightly lower than the measured toughness for the thin specimen. Overall, equation (2) appears to have reasonable validity among DRA materials. The only difficulty occurs when predicting the toughness for a peak aged material. In that condition, the material is prone to shear band localization, and an alternate formulation is necessary. The reader is referred to [7] for further details on toughness modeling of DRAs where shear localization is present, under the condition that the DRA has a reasonably uniform distribution of particles.

One can use a crack bridging model with ductile ligaments to model the toughness of the DRA with the ductile Al particles. A simple Dugdale model gives:

$$K_{bridging} = 2f\sigma_y^{Al}\sqrt{2L/\pi} \qquad (3)$$

where f is the volume fraction of the bridging phase, σ_y^{Al} is the flow stress of the Al, and L is the length over which the crack is bridged. At crack initiation, L is small (maximum 0.5 mm). Assuming a flow stress of 100 MPa for the pure Al ligament, the toughness improvements are 0.35 MPam$^{1/2}$ and 0.9 MPam$^{1/2}$ for the materials with 10 volume percent and 25 volume percent Al particles, respectively. The data for the 25 percent particles are clearly greater than the predicted values, and an alternate model is necessary.

A more likely mechanism of toughening of this DRA is crack trapping, which does not require that the crack propagate with isolated islands of ligaments left behind. We use here the model of Bower and Ortiz [9]:

$$\frac{K_{max}}{K_{matrix}} = \left\{(1-\sqrt{f}) + (2.1 + 2.4\sqrt{f})\sqrt{f}\right\}^{1/2} \qquad (4)$$

where K_{max} is the maximum toughening achievable, and K_{matrix} is the toughness of the matrix. Here, we identify K_{matrix} with the toughness of the control DRA (i.e., 16 MPam$^{1/2}$), and f with the volume fraction of the ductile Al phase. The ratio in equation 4 is calculated to be 1.26 and 1.47 for the 10 percent and 25 percent materials, respectively. Equation 4 should certainly be applicable in the steady state domain. Using the steady state toughness (K_{ss}) of 20 MPam$^{1/2}$ for the control DRA, we obtain K_{ss} of 25 MPam$^{1/2}$ and 29.4 MPam$^{1/2}$ for the two volume percent Al particles. These may be compared with experimental values of 25 MPam$^{1/2}$ and 34 MPam$^{1/2}$. The bridging effect also plays a role in K_{ss}. If we assume a total ligamented crack of 3 mm, in keeping with the observed R-curve data, the combined effects from equation (3) and (4) are K_{ss} of 25.9 MPam$^{1/2}$ and 31.6 MPam$^{1/2}$ for the two materials. These are in excellent agreement with the observed data. Overall, the largest contribution to K_{ss} appears to be from crack trapping than crack bridging.

We can extend the crack trapping model to predict initiation toughness. Using the initiation toughness of 16 MPam$^{1/2}$ for the control DRA, we calculate the initiation toughness for the 10% and 25% ductile phase toughened materials as 20 MPam$^{1/2}$ and 23.5 MPam$^{1/2}$, respectively. These may be compared with the experimental data.

STABILITY ANALYSIS

A J-R curve becomes useful only under conditions of stable fracture, when:

$$J_{app}(a) = R(a) \qquad (5a)$$

$$\frac{dJ_{app}}{da} \leq \frac{dR}{da} \qquad (5b)$$

where J_{app} is the driving force, obtained from elastic-plastic analysis, and R characterizes the material's resistance to crack growth. While equation 5(a) is independent of whether loading is load or displacement controlled, dJ_{app}/da does depend on the particular type of loading. Displacement control is more stable, since the driving force generally decreases with crack length at constant displacement. This stability aspect has been exploited in leak-before-break calculations of steel pipes used in power generation, where loss of steam pressure through cracked regions of the pipe reduce the diving force for crack growth. Such applications are unlikely with DRA materials.

In order to evaluate the stability of DRA materials, which possess limited J_{Ic} and dR/da, we consider a center cracked tension (CCT) panel under load control. The latter is considered because many anticipated applications are in load control: fan blades and fan exit guide vanes in aerospace turbine engines, ventral fins in fighter planes, door-hatch in airplanes (internal pressure), etc. As indicated earlier, similar load controlled conditions are also likely to be present in applications of high temperature intermetallics, which also possess limited fracture toughness and crack resistance behavior. Thus, the analysis is anticipated to have general usefulness. The reason a CCT panel was considered is because this geometry produces the slowest increase of J with crack length, compared to other geometry. We used a plane stress formulation; to give the specimen added stability.

A CCT specimen with a total width, 2W=20mm, total length L=100 mm, and thickness B=2mm, was considered. Plane stress conditions were assumed. Two different initial crack lengths (total length $2a_o$) were considered: $2a_o$=12 mm and $2a_o$=0.4 mm. The rationale was to vary the plasticity component. Thus, the specimen having the shorter crack length (a_o=0.2 mm) would have a larger plasticity component at crack initiation (i.e., P/P_o closer to unity, where P_o is the limit load equal to the ligament area times the yield strength) compared with the specimen with a_o=6mm. Load-displacement and J values were generated for these two specimens using standard elastic and EPRI's plastic estimation formulas. Effective crack lengths were determined using an iteration method and employing Irwin's plasticity correction. Different crack lengths (a) were considered, starting from the initial a_o and up to a_o+3mm, the typical value where steady-state conditions were observed; see Figure 3. At the loads corresponding to crack initiation for the control DRA (~16 $MPam^{1/2}$) and the DRA with 25 percent large Al particles (~20 $MPam^{1/2}$), dJ/da was computed at constant load.

The applied J versus crack growth (Δa) from elastic plastic computations of the CCT specimen are compared with experimental data in Figure 4. The constant load curves 'a' and 'b' correspond to a_o of 6 mm and 0.2 mm, respectively, and are calculated based on the load at crack initiation (J_{Ic}=2.8 kJ/m^2). The P/Po values at crack initiation were 0.39 and 0.54 for curves 'a' and 'b', respectively. For both these crack lengths, dJ/da at constant P was larger than dR/da (from experimental data). Thus, both the CCT specimens would be unstable at crack initiation.

Figure 5 illustrates the load-elongation curve that would be generated on the CCT specimen with 6 mm crack length, if the material follows the J versus crack length curve generated from the experiments. This plot clearly shows that the maximum load is reached at crack initiation, and that both the load and displacement would have to decrease if the R-curve of the material was to be followed. The maximum load is reached at crack initiation, indicating that instability would ensue at crack initiation, and that the rest of the R-curve would not be of any significant value.

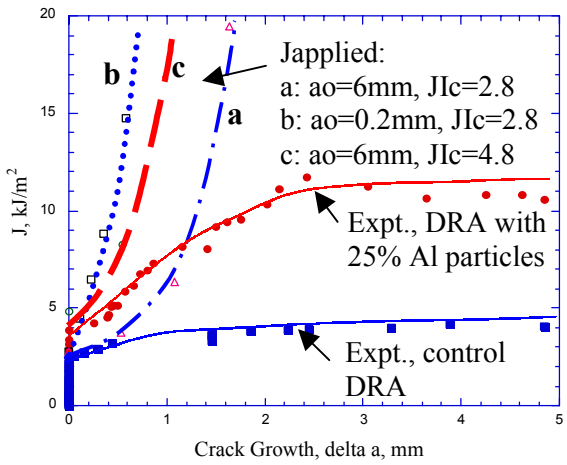

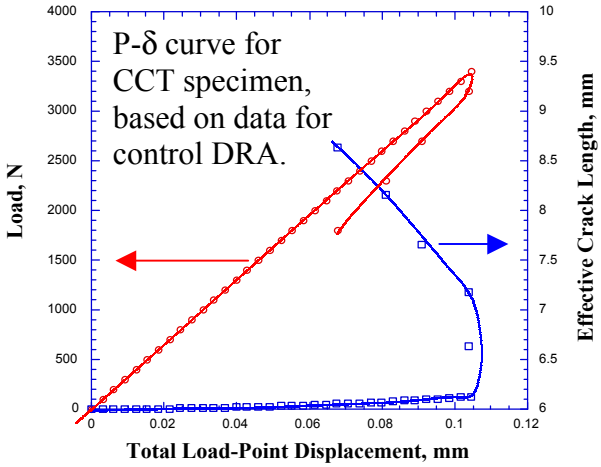

Figure 4. J versus crack growth for a CCT specimen under plane stress, and experimental data (R-curves) for the two DRA materials. The crack lengths used in the calculations are indicated.
Figure 5. Load vs displacement and load vs crack length for the CCT specimen, based on data from the control DRA.

Returning to Figure 4, the curve marked 'c' corresponds to $J_{applied}$ versus Δa at constant load, where the load is based on crack initiation at Keq=20 $MPam^{1/2}$; a_o is 6 mm. This Keq corresponds to the initiation toughness of the ductile phase toughened material with 25 percent large Al particles. Recall from Figure 3 that this material exhibited one of the highest dJ/da. Figure 4 once again illustrates that the $J_{applied}$ curve, 'c', deviates from the R-curve from the point of crack initiation (dJ/da>dR/da), indicative of instability at crack initiation. Thus, although this material had significantly improved crack growth resistance, the enhancement appears to be inadequate for maintaining component integrity under load controlled conditions. Overall, the main problem appears to be the low dJ/da, which results in tearing modulus values $\{T=(E/\sigma_y^2)*dJ/da\}$ in the range of 0.5 to 1.1 for the current composites. These values may be compared with T ranging between 20 and 200 for structural steels. It appears therefore that significant improvements in dJ/da will be necessary before the R-curves can be put to use for DRAs and intermetallics, which have limited ductility.

It is acknowledged that dJ/da at constant load is too stringent in terms of applications, and that a system compliance should be incorporated into the stability analysis. On the other hand, rotating components in turbines are often under load control. Static components offer greater flexibility, and some advantage may be gained from the R-curve behavior. However, we have conducted stability analysis using some typical machine compliance (C_M) values. Although those results are not reported here, they do indicate that the T values are too low to be of much usefulness. Moreover, steady-state toughness values impose added limitations, and these show up better in a plot of T versus J. Our conclusion is that at least an order of magnitude increase in dJ/da is necessary before R-curves become useful for such materials.

CONCLUSIONS

Experiments were conducted on a control DRA, and DRAs toughened extrinsically with Al-particles. The following conclusions are obtained:

a) In these materials, the crack grows primarily under small scale yielding conditions. The appropriate method to determine the J-R curve is discussed.

b) The Al-particles have a greater effect on steady state toughness than the initiation toughness. A good prediction of the toughness of the ductile phase toughened material is obtained through a crack-trapping model.

c) Stability analysis, using the material data and a CCT specimen geometry, indicate that the current dR/da values are insufficient to prevent instability at crack initiation, under load controlled conditions. A significant improvement in the tearing modulus is necessary before the R-curve behavior can be utilized in such materials of limited ductility.

ACKNOWLEDGMENTS

This work was partially funded under a collaborative NUCOR program with the Los Alamos National Laboratory. Part of the work was conducted while the author was at the Wright Laboratories, AFRL, Ohio. Discussions with Dr. A.B. Pandey at Pratt & Whitney, and Dr. D.B. Miracle at AFRL, are gratefully acknowledged.

REFERENCES

1. Pandey, A.B., Majumdar, B.S., and Miracle, D.B. (2000) *Metall. Trans.*, *31A*, pp.921-936
2. Lewandowski, J.J., Liu, C., and Hunt, W.H. Jr. (1989) *Mater. Sci. Eng.*, *107 A*, 241
3. Pandey, A.B., Majumdar, B.S., and Miracle, D.B. (1999) *Mater. Sci. Eng.*, *259 A,* pp.296-307
4. Kumar, V., German, M.D., and Shih, C.F. (1981) *Electric Power Research Institute, EPRI NP 1931*
5. Anderson, T.L. (1995) *Fracture Mechanics: Fundamentals and Applications*, CRC Press LLC
6. Rice, J.R. (1968) *J. Appl. Mech.*, *35*, p. 379
7. Majumdar, B.S., and Pandey, A.B. (2000) *Metall. Trans., Vol. 31A*, pp.937-950
8. Pandey, A.B., Majumdar, B.S. and Miracle, D.B. (1998) *Metall.Trans. A* , *29 A*, pp.1237-1243
9. Bower, A.F., and Ortiz, M. (1990) *J. Mech. Phys. Solids, 38*, p.443